ELSEVIER

Journal of Nuclear Materials 273 (1999) 37–51

journal of nuclear materials

www.elsevier.nl/locate/jnucmat

Kohler solution model for prediction of activities of constituent metals in austenitic steels and other iso-structural alloys and a comparison with experimental data

H.P. Nawada, O.M. Sreedharan *

Thermodynamics and Kinetics Division, Materials Characterisation Group, Indira Gandhi Centre for Atomic Research, Kalpakkam, Tamil Nadu 603 102, India

Received 17 August 1998; accepted 6 January 1999

Abstract

A thermodynamic model based on sub-regular solution was utilised to facilitate prediction of high temperature activities of constituent elements in austenitic stainless steels and other iso-structural alloys. Nearly 95 interaction parameters needed for the computations were also compiled from the literature. The model was utilised for computing activities of a few major metallic components such as Fe, Cr, Ni, Mo and Mn in most of the austenitic stainless steel series. A comparison was made between the activities predicted by the model and those reported from the available literature which were based on Knudsen cell mass spectrometry and metastable EMF methods, essentially on some Fe–Cr–Ni alloys and stainless steel type AISI 304 and 316. The possible reasons for the mismatch in the values of activities were discussed. The application of the model for simulation studies involving variation of composition with respect to one solute element was also presented.

1. Introduction

Austenitic stainless steels are finding extensive applications as structural materials. Even among austenitic stainless steels there are quite a few varieties which are either in use or under development. Some of the modifications in their compositions were made mostly for improvement in specific mechanical properties and occasionally for economic reasons aimed at minimising the use of Cr and Ni. These stainless steels contain a wide spectra of elements in the periodic table including the ones added intentionally as well as those which are unwanted impurities. The criterion for the choice of structural alloy is the compatibility of the constituents of the alloys with the local environment. In this context, the activities of metals in such stainless steel materials are of profound importance. One way of obtaining the activities of constituents in these alloys is by measuring them with a suitable experimental technique. However, it is not experimentally feasible to measure the activities of all the elements; but determining some and deducing the others by resorting to Gibbs–Duhem type integration warrant preparation of synthetic alloys with wide variations in compositions which are infeasible. This experimental approach is further compounded by the lack of uniqueness of the composition of the commercial alloys which are invariably expressed as a range such as Cr-16–18 wt% for Cr. This makes the activities measured on one batch of alloy material not adoptable for another batch without reservation owing to compositional variations. Further, the activity of a particular element is not merely dependent on the concentration of that specific constituent element alone, but also is dependent on those of other elements. Structural materials in nuclear reactor might also undergo radiation induced segregation resulting in the manifestation of compositional changes at least in some locations.

These compositional changes could either be modest enrichments/depletions of some constituent elements, or drastic changes in the composition resulting in

* Corresponding author. Tel.: +91-4114 40202; fax: +91-4114 7360; e-mail: oms@igcar.ernet.in.

0022-3115/99/$ – see front matter
PII: S0022-3115(99)00019-7

Table 1
Binary interaction parameters (in units J/mol) for most of the SS-related binary alloys. The key to the use of A and B terms from this table in Eqs. (1) and (2) is illustrated below:

$G_{\mathrm{fcc}}^{\mathrm{Ex}}(\mathrm{Fe,Mo}) = (x_{\mathrm{Fe}} \times x_{\mathrm{Mo}})/(x_{\mathrm{Fe}} + x_{\mathrm{Mo}}) \times \{x_{\mathrm{Fe}} \times (24790 - 8.368 \times T) + x_{\mathrm{Mo}} \times (25376 - 8.368 \times T)\}$

i		*j*																
		Fe	Ni	Cr	Mo	Mn	Ti	Si	C	Nb	Ta	Al	Co	W	Cu	V	Zn	N
Fe	A		Refer	7116.2	24790	−18870	−33472	−136817	−94558	0	32217	50650.6	Refer	42258	36700	−18180	12562	−14267
	B		Table 2	−6.279	−8.368	16.987		7.95	−2.929			14.2324	Table 2	−12.761	−0.949	1.16	−1.995	
Ni	A	Refer		Refer	−13604	−64434	−182422	−264345	−79496	−148532	−127558	Refer	Refer	−29288	11632			
	B	Table 2		Table 2	13.8138	10.878	54.39	62.01	4.31			Table 2	Table 2	20.92	0.2092			
Cr	A	7116.2	Refer		34309	−17573	25104	−81558	−74475	29288	−1255	−60250	4602	31380	104600			10000
	B	−6.279	Table 2		−11.3	10.46		−37.656	−121.3				−31.38					
Mo	A	25376	−13604	21338		0	5192	−61923	−37656	−23027		−16736	−25104					−26132
	B	−8.368	13.8138	−5.86								12.552	20.82					
Mn	A	−18870	−64434	−17573		0	−2720	−104184	−141419		−4184	−69036	−23849		18200	−11820		−74116
	B	16.987	10.878	10.46				−23.012	−4.602			22.761						13.9
Ti	A	−10460	−90374	12552	5192	−2720			−288696	13075	6000	−101253	−111294	16318	4602	14000		
	B		29.29						41.84			41.84	29.29	7.95				
Si	A	−304177	−138238	−106692	−61923	−8409			0	−280328	0	34978	−141419	−15859	138365			5000
	B	136.817	22.01	29.288		2.092						−41.17	32.01		−96.232			
C	A	−155226	−10784	−74475	−37656	−288278	−288696	0		−169034	−155465	−78659	−9581	16736				
	B	5.816	67.7	−121.34		47.698	41.84			−20.92	20.92		6.02					
Nb	A	0	−48116	22594	−23027		13075	−115060	−169034	0		−213384	−7113		98742	9080		
	B								−20.92			67.781			−41.85			
Ta	A	−14225	−99567	8368	0		5000	0	−155465	0		−188949	−6000	−290000	104600	6929		
	B								20.92			62.76						
Al	A	−154882	Refer	−60250	−16736	−48116	−101253	25773	−78659	−213384	−188949		−104600	−23849	−6736			
	B	71.162	Table 2		−12.552	22.761	41.84	−41.17		67.781	62.76			26.15	0.711			
Co	A	Refer	Refer	−8786	−25104	−23849	−155266	−209618	−59831	−7113	−90000			−4602	29288			
	B	Table 2	Table 2	−31.38	20.92			54.31	32.01	−11.07				10.46				
W	A	45020	41480	28023			16318	−15859	16736		300000							
	B	−1.883																
Cu	A	−11400	2469	104600		5021	4602	−230245		98742	104600					56136		
	B	18.591	4.058					96.232		−41.84						−3.519		

Table 1 (Continued)

i		j														
		Fe	Ni	Cr	Mo	Mn	Ti	Si	C	Nb	Ta	Al	Co	W	Cu	V	Zn	N
V	A	−18180				−11820	13500			9080	6929							−65500
	B	1.16																23.55
Zn	A	−15174																
	B	1.995																
N	A	−14267		10000	−26132	−74116		5000										
	B					123.9												

precipitation of certain phases depending on the extent of irradiation besides temperature and other metallurgical factors. The precipitates formed may/may not have the fcc structure of the parent austenitic phase. Nevertheless, the small changes in composition by way of enrichments/depletions might still be accommodated in the austenitic phase within some limits as dictated by the phase diagram. The activity of each constituent element as a function of all other elements in stainless steels and related alloys is a multi-dimensional problem. The solution to this problem is only a thermodynamic model which can predict activities of each element in stainless steel materials and which is duly validated with the available experimental data.

2. Thermodynamics of the model

There are a large number of investigations on thermodynamic modelling of stainless steel related materials chiefly generating vast sources of information on thermodynamic parameters as well as optimisation of thermodynamic data against the available phase diagrams [1,2]. However, these investigations are primarily related to the development of phase diagrams of such materials. In this regard, a simple solution model which is capable of predicting the thermodynamic activity of every solute element has been attempted. The present model assumes the austenite phase to be a fcc solid solution of n components, where the maximum value of n is 17 which can include elements such as Fe, Ni, Cr, Mo, Mn, Ti, Si, C, Ta and Nb. More elements viz., W, Al, Cu, V and N could also be added to the system with limited terms. The integral molar Gibbs' energy of the austenitic phase ${}^{\circ}G^{\mathrm{fcc}}$ utilising the Kaufman approach [3] is given by

$$ {}^{\circ}G^{\mathrm{fcc}} = \sum_i x_i \, {}^{\circ}G^{\mathrm{fcc}} + RT \sum_i x_i \ln x_i + \sum_i \sum_{j \neq 1} x_i x_j / (x_i + x_j) \times (\Omega_{i,j} \times x_i + \Omega_{I,i} \times x_j), \tag{1} $$

where ${}^{\circ}G^{\mathrm{fcc}}$ is the Gibbs energy of a pure component i for the fcc phase at the temperature of interest, $\Omega_{i,j}$ and $\Omega_{j,i}$ are interaction parameters of any two elements and x_i is the atomic fraction of component i in the austenitic phase (fcc).

Even though, there are various methods for obtaining excess Gibbs energy terms for a given multi-component solution from the ones available for the binaries [4], a Kohler sub-regular solution-type approach was chosen. The fcc phase wherein some of the elements such as carbon (and nitrogen) which occupy interstitial positions may be approximated to a substitutional solution. Perhaps, a better approach would be to consider sub-lattice model developed by Hillert and Staffansson [5] for an accurate evaluation of activities. Since the

Table 2

	System i–j	Binary interaction parameters (in units of J/mol)		Temp. range (in K)
		$\Omega_{i,j}$	$\Omega_{j,i}$	
1	Fe–Ni	$(2093 - T^2 \times 3.833\ \mathrm{E}-03 + T^3 \times 1.6337\ \mathrm{E}-06)$	$(-34827.52 + 2.441568\ \mathrm{E}-03 \times T^2 + T^3 \times 1.0406\ \mathrm{E}-06)$	0–1800
2	Fe–Co	$(-2322 + 2.0849\ \mathrm{E}-03 \times T^2 - 4.2941\ \mathrm{E}-07 \times T^3)$	$(-983 + 5.7333\ \mathrm{E}-03 \times T^2 - 1.1811\ \mathrm{E}-06 \times T^3)$	
3	Ni–Cr	$(-25116 + 0.009482 \times T^2 - 2.6083\ \mathrm{E}-06 \times T^3)$	$(-25116 + 9.4817\ \mathrm{E}-03 \times T^2 - 2.6083\ \mathrm{E}-06 \times T^3)$	800–1800
4	Ni–Al	$\{(-189987 + 0.13924 \times T^2 - 2.7313\ \mathrm{E}-05 \times T^3 - 149.452 \times T)\}$	$\{(-19907 - 0.13924 \times T^2 - 2.7313\ \mathrm{E}-05 \times T^3 - 182.506 \times T)\}$	300–2000
5	Ni–Co	$(+4602 - 5.3815\ \mathrm{E}-03 \times T^2 + 2.8698\ \mathrm{E}-06 \times T^3)$	$(+4602 - 5.3815\ \mathrm{E}-03 \times T^2 + 2.8698\ \mathrm{E}-06 \times T^3)$	0–1000
6	Al–Co	-104600	$(-16730 + 266.868 \times T - 0.3609 \times T^2 + 1.3277\ \mathrm{E}-06 \times T^3)$	300–3700

E$-0X$ stands for $\times 10^{-0X}$.

concentrations of these elements (C and N) are very low in most of the commercial austenitic alloys and the present model is primarily delaing with major alloying elements, the difference in the computed values of configurational entropy as well as excess Gibbs energy between the sub-regular and sub-lattice models corresponding to these elements could be deemed to be negligible. However, development of model focusing on activity of minor elements namely C, or N or B, it is prerequisite to consider sub-lattice model. In this sub-regular Kohler solution approach the interaction parameters were temperature-dependent and asymmetric with respect to solute concentrations. This choice was made owing to the availability of systematic, exhaustive and comprehensive compilation of data on stainless steel-related materials by Kaufman and his coworkers which were published extensively in Calphad journal. The partial molar Gibbs excess free energy of component i in the austenite phase is

$$\begin{aligned} RT\ \ln\ \gamma_i = & \sum_i bx_{(j,i)} \times \{bx_{(j,i)} + 1 - x_i\} \times \Omega_{i,j} \times x_i \\ & + \sum_{j \neq i} \{bx_{(j,i)}^2 - x_i \times bx_{(j,i)}\} \times \Omega_{j,i} \times x_j \\ & - \sum_{j \neq i} \sum_{k \neq j} bx_{(j,k)} \times x_k \\ & \times \{\Omega_{j,k} \times x_j + \Omega_{k,j} \times x_k\}, \end{aligned} \tag{2}$$

where $bx_{(j,i)} = x_j/(x_i + x_j)$, $bx_{(j,k)} = x_j/(x_j + x_k)$ and γ_i is the activity coefficient. The activity of a particular element a_i could be calculated by multiplying γ_i with the respective molefraction x_i.

The binary fcc interaction parameters used are summarised in Tables 1 and 2. The key to the literature for the data summarised in Tables 1 and 2 could not be incorporated in the table itself to avoid the loss of clarity. Hence, the relevant references are encoded in the usual manner following each binary system: Fe–Ni [6], Fe–Cr [7,22,25], Fe–Mo [8,34], Fe–Mn [9,10], Fe–Ti [9,36], Fe–Si [10,35], Fe–C [11], Fe–Nb [8], Fe–Ta [13], Fe–Al [14,15], Fe–Co [8], Fe–W [13,29], Fe–Cu [14], Fe–V [15], Fe–Zn* [16], Fe–N [17], Ni–Cr [6], Ni–Mo [12], Ni–Mn [12], Ni–Ti [18], Ni–Si [10], Ni–C [11], Ni–Nb [18], Ni–Ta [19], Ni–Al [6,19], Ni–Co [18], Ni–W [18], Ni–Cu [6], Cr–Mo [32], Cr–Mn [11], Cr–Ti* [8], Cr–Si [13,33], Cr–C [20], Cr–Nb [8], Cr–Ta* [13], Cr–Al* [19,32], Cr–Co [8], Cr–W* [8], Cr–Cu [16], Cr–N [21], Mo–Mn [32], Mo–Ti [18], Mo–Si [10], Mo–C [16], Mo–Nb [22,33], Mo–Al* [19], Mo–Co [18], Mo–N [21], Mn–Ti [12], Mn–Si [13], Mn–C [11], Mn–Ta [13], Mn–Al [22], Mn–Co [22], Mn–Cu [10], Mn–V [23], Mn–N [17], Si–C [24], Si–Nb [10], Si–Ta* [13], Si–Al [10], Si–Co [10], Si–W* [10], Si–Cu [28], Si–N [25], Ti–C [11], Ti–Nb* [12,31], Ti–Ta* [13], Ti–Al [19], Ti–Co [18], Ti–W* [10], Ti–Cu [10], Ti–V* [26,31], C–Nb* [11], C–Ta [13], C–Al [20], C–Co [18], C–W [10], Nb–Ta [27], Nb–Al* [19], Nb–Co [18], Nb–Cu [10], Nb–V* [26], Ta–Al* [13], Ta–Co [13], Ta–W* [13], Ta–Cu [13], Ta–V* [13], Al–Co [8], Al–W* [19], Al–Cu [19], Co–W [18], Co–Cu [19], Cu–V [28], V–N [23,30], V–Nb* [30] and V–Ta* [13]. (The superscript (*) indicates the use of data on bcc phase wherever the corresponding fcc data were not available.) Though interaction parameters for binaries with N are given in the Table 1 we have not used the terms pertaining to binary systems of N in the present calculations. The partial molar Gibbs energies are calculated using numerical differentiation of Eq. (1) as well. The values of $^\circ G_i$ are selected from SGTE [37]. The model assumes that for any given composition, the whole system remains as a single fcc phase that is the austenitic phase. The present model considers only binary interaction parameters. Since the basic data used for the calculations are temperature dependent and concentration asymmetric binary interaction parameters $\Omega_{i,j}$ and $\Omega_{j,i}$, the estimation may not be very accurate. However, inclusion of higher order interaction parameters viz., ternary interaction parameters $\Omega_{i,j,k}$ will be attempted in our later work as it involves more rigorous mathemati-

Table 3
Predicted activity coefficients for the major elements in the temperature range 750–1750 K fitted into the following mathematical form:

$\gamma_i = A + B \times T + C \times 1000/T + D \times 10^{-6} \times T^2$

Material	Element	A	B	C	D
SS301	Fe	0.8932	4.32E−05	0.2729	−0.0023
	Ni	−0.2090	9.43E−04	−0.0368	−0.2542
	Cr	0.0512	3.57E−04	0.6146	−0.0822
	Mn	−2.1617	2.44E−03	0.5553	−0.3111
SS302	Fe	0.8444	5.50E−05	0.3282	−0.0006
	Ni	−0.4007	1.12E−03	0.0126	−0.3119
	Cr	0.1805	2.93E−04	0.5212	−0.0686
	Mn	−2.0538	2.25E−03	0.5400	−0.2670
SS304	Fe	0.8993	1.23E−05	0.2442	0.0105
	Ni	−0.3235	1.10E−03	−0.0120	−0.3192
	Cr	0.3414	2.31E−04	0.4304	−0.0556
	Mn	−2.1180	2.23E−03	0.5741	−0.2410
SS304L	Fe	0.8249	4.80E−05	0.3269	0.0033
	Ni	−0.5105	1.20E−03	0.0445	−0.3359
	Cr	0.2846	2.63E−04	0.4802	−0.0620
	Mn	−1.9979	2.18E−03	0.5260	−0.2530
SS310	Fe	0.4705	1.42E−04	0.6057	0.0108
	Ni	−0.9588	1.59E−03	0.1725	−0.4656
	Cr	0.2933	3.64E−04	0.6367	−0.0804
	Mn	−1.1977	1.11E−03	0.3510	−0.0187
SS316	Fe	0.7499	7.62E−05	0.4072	0.0021
	Ni	−0.6240	1.32E−03	0.0732	−0.3745
	Cr	0.3573	2.12E−04	0.3892	−0.0530
	Mo	−52.4394	3.65E−02	29.0127	−8.5121
	Mn	−1.8468	1.96E−03	0.4969	−0.2056
SS316LN	Fe	0.7562	6.92E−05	0.3928	0.0035
	Ni	−0.6246	1.32E−03	0.0743	−0.3723
	Cr	0.3716	2.14E−04	0.3929	−0.0536
	Mo	−51.2161	3.56E−02	28.3800	−8.3097
	Mn	−1.8520	1.97E−03	0.4967	0.208
SS321	Fe	0.7894	6.65E−05	0.3738	0.0011
	Ni	−0.5189	1.23E−03	0.0448	−0.3464
	Cr	0.2494	2.70E−04	0.4826	−0.0646
	Mn	−1.9519	2.11E−03	0.5186	−0.2358
SS347	Fe	0.7872	6.53E−05	0.3756	0.0021
	Ni	−0.5378	1.25E−03	0.0497	−0.3529
	Cr	0.2780	2.57E−04	0.4633	−0.0616
	Mn	−1.9406	2.08E−03	0.5179	−0.2289
D9	Fe	0.6936	7.85E−05	0.4510	0.0101
	Ni	−0.7184	1.45E−03	0.0947	−0.4201
	Cr	0.4117	2.00E−04	0.3589	−0.0551
	Mo	−47.5441	3.30E−02	26.6817	−7.6796
	Mn	−1.7511	1.75E−03	0.4911	−0.1378
INCONEL	Fe	−1.6088	2.23E−03	0.3642	−0.6723
	Ni	1.2091	−8.88E−05	0.0400	−0.0372
	Cr	0.2815	4.18E−04	−0.1308	−0.1530
	Mo	1.5012	5.00E−04	−0.6648	0.1321

Table 3 (Continued)

Material	Element	A	B	C	D
NIMONIC	Fe	0.7395	3.00E−04	−0.0052	−0.0722
PE 13	Ni	0.9090	3.16E−04	−0.2753	−0.1725
	Cr	0.7505	1.10E−04	−0.1381	−0.0655
	Mo	1.3132	−2.71E−04	1.0169	0.2866
PE 16	Fe	0.2751	2.31E−04	0.7605	0.0154
	Ni	−0.2038	1.22E−03	−0.0589	−0.3943
	Cr	0.8032	−2.65E−06	0.0658	−0.0424
	Mo	−8.1816	5.82E−03	6.8549	−1.1480
USPCA	Fe	0.7635	3.48E−05	0.3798	0.0208
	Ni	−0.6082	1.38E−03	0.0624	−0.4054
	Cr	0.5095	1.48E−04	0.2622	−0.0473
	Mo	−42.6126	2.96E−02	24.1691	−6.8632
	Mn	−1.6383	1.58E−03	0.4711	−0.1018

E−0X stands for $\times 10^{-0X}$.

cal and cumbersome treatment. These $\Omega_{i,j}$ terms for many stainless steel related binary systems have been critically assessed by Kaufman et al., during the last two decades. The improvement is not only in the accuracy of some of the critical data needed, but also in the inclusion of contributions by many 'minor' constituents (designated as minor owing to their presence in very small concentrations) in terms of major–minor and minor–minor interaction energies. These additional terms also play a role in a cumulative manner in altering the activity coefficients of a particular element. Such methods of estimation were attempted earlier for Fe–Cr–Ni ternary alloys by earlier workers. Though extensive modelling of multi-component systems could be located in the literature, but these models are mostly used for construction of phase diagrams and not specifically used for prediction of activities of constituent elements in multi-component systems such as stainless steels.

3. Comparison of predicted activities with experimental data

The above Eqs. (1) and (2) are utilised to predict activity coefficients γ of major elements such as Fe, Ni, Cr, Mo, Mn, C and Si of stainless steels and other isostructural alloys. The γ_s so calculated are represented in a polynomial form for the sake of brevity. The values of γ_s for some of the above-mentioned elements in the austenitic stainless steels of the type AISI, 301, 302, 304, 304L, 310, 316, 316L, 321, 347 and D9, USPCA as well as Ni rich alloys such as PE13, PE16 and Inconel are tabulated in Table 3. The compositions for the above materials [38] which are chosen for calculations are listed in Table 4. The composition of AISI 304, 316, 316LN and D9 are selected from a recent thermodynamic measurement report by Azad et al. [39]. Whenever the composition was given in the literature, it uses invariably represented as a range, the mean value of which was chosen for the calculations. To evaluate the method of prediction, the calculated activities are compared with the experimental data wherever available in the literature. The results of comparison are grouped into the following four Sections 3.1–3.4.

3.1. Comparison of Fe–Cr–Ni ternary with small additives

The experimental activities for these ternary systems are primarily from mass spectrometry [40–43]. According to Gibby and St. Pierre [39] the activity coefficients of Fe, Cr and Ni at 1873 K were 1.03, 1.20 and 0.52, respectively, for Fe-20 Cr-10.2 Ni (at.%) ternary alloy. Based on the evaluation of experimentally obtained data by Belton and Fruehan [41] the activity-coefficients for Fe, Cr and Ni at 1873 K were evaluated to be 1.00, 1.09 and 0.77, respectively. The predicted values for activity coefficients γ_s were 1.043, 0.839 and 0.625, respectively which were relatively close to the later experimental values. However, the predicted activities were found to be in fair agreement with the experimental activities of Cr and Ni reported by Lee [43] who studied the effect of Al and Si additions to a Fe–Cr–Ni ternary alloy by measuring their vapour pressures using K-cell mass spectrometry (KCMS). Even though the experimental data on a_{Fe} were found to be in the same range as those for the pure ternary alloy (see Fig. 1), the observed trend with respect to some of its additives such as Si was significantly different. However, the model predicted for activity of Cr and Ni is somewhat closer to the corresponding experimental results. Further, Lee observed that by adding small amounts of Si to the quaternary alloy Fe–Cr–Ni–Al (the concentration of Al being quite small) the activities of Fe, Cr and Ni were observed to decrease marginally in contrast with the diverse behav-

Table 4
The compositions (in at.%) of various stainless steels. The compositions for the SS types 304,316 and 316LN are mentioned more than once owing to slight differences in the composition of the same type of stainless steels used by different authors

Material	C	Si	Mn	Cr	Ni	Mo	Fe	Other minor elements
SS301	0.6806	1.9386	1.982	17.80	6.492		70.976	
SS302	0.6807	1.9390	1.983	18.85	8.348		68.067	
SS304	0.3639	1.9434	1.987	19.95	9.297		66.334	
SS304L	0.1367	1.9468	1.991	19.98	9.313		66.501	
SS310	1.1310	1.9329	1.976	26.10	18.956		49.772	
SS316	0.3685	1.9682	2.012	18.07	11.299	1.440	64.707	
SS316L	0.1384	1.9718	2.016	18.10	11.319	1.443	64.873	
SS321	0.3657	1.9529	1.997	18.99	9.809		66.757	
SS347	0.3672	1.9611	2.005	19.07	10.320		66.149	
PE16	0.2333	0.2193		18.41	40.528	1.838	34.716	Ti = 1.36; Al = 0.27
USPCA	0.2304	0.8015	1.803	15.02	15.429	1.803	65.124	Ti = 0.28
D9	0.1623	1.6064	0.842	16.71	14.610	1.393	64.228	Ti = 0.49
SS304	0.2010	1.3677	1.029	19.10	9.253		68.950	Azad et al. Ref. [39]
SS316	0.2835		1.890	18.09	11.553	1.373	66.626	Ref. [39] N = 0.12
SS316LN	0.1159	0.5450	1.783	19.11	11.490	1.421	65.109	Ref. [39] N = 0.28
SS316	0.361	1.07	1.79	17.25	13.20	1.413	64.10	Koyama et al. Ref. [47] Ti = 0.116; Al = 0.033; N = 0.067
SS316	–	0.2700	3.540	22.52	9.410	2.290	61.910	Venugopal et al. Ref. [48] Cu = 0.058
SUS304L	0.101	1.1400	0.960	19.430	9.320	0.030	68.823	Hirai et al. Ref. [44] N = 0.10; Cu = 0.04
Alloly 617	0.34	0.17	0.02	24.94	53.86	5.51	0.16	Hilpert Ref. [50] Co = 12.3; Al = 2.28; Ti = 0.42
PE-13	0.32	0.73	0.43	23.70	48.90	5.60	18.90	Ref. [50] Co = 1.5
IN-643	2.47	0.95		28.56	48.01	0.37	3.19	Ref. [50] Co = 12.1 W = 2.83; Ti = 0.19; Zr = 0.07; Nb = 1.28

iour predicted by the model for Si additions (Fig. 1). The measurements by Lee were made at very high temperatures where the problems of compatibility between the sample and the cell material could be rather severe. However, no mention of the cell material or its liner was made in the paper by Lee even for an assessment of compatibility. The reasons for disagreement between the predicted activities with those by KCMS would be discussed in detail in the subsequent sections.

3.2. Comparison of SS304 and other related materials

Hirai et al. [44] had measured activities of Fe,Cr and Mo in a material which is equivalent to SS304 (represented as SUS 304 by the authors) by using KCMS over the temperature range 1000–1430 K with K-cell made of Mo. In addition they employed LiCl as an internal standard for the temperature calibration besides its serving the purpose of alignment of the K-cell. The alloy

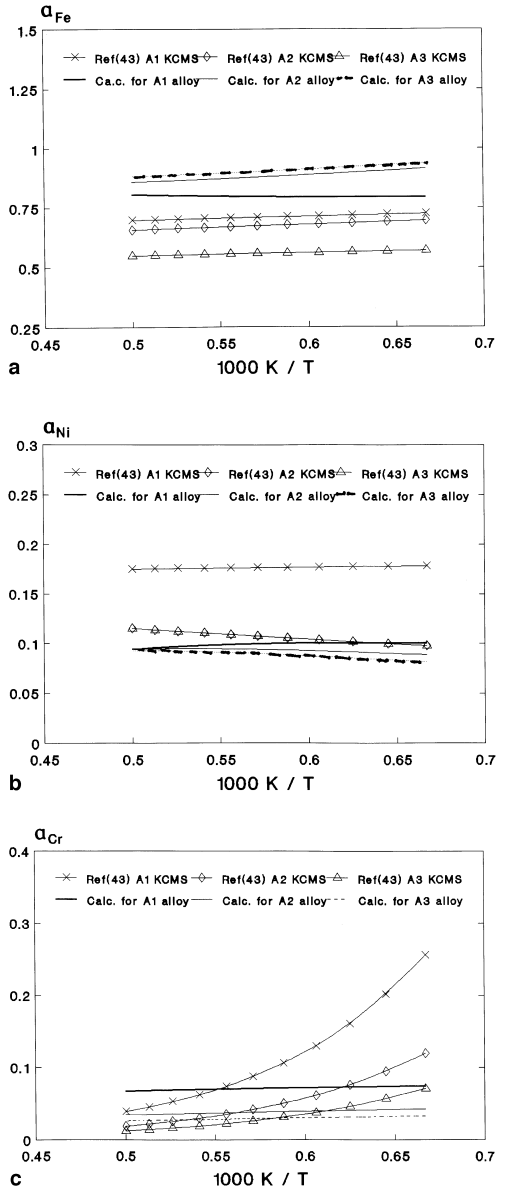

Fig. 1. Comparison of computed activity-coefficients in ternary Fe–Cr–Ni system with small additions of Al and Si with experimental data by Lee [43] obtained by employing KCMS: (a) for Fe, (b) for Cr and (c) for Ni. Compositions of alloys taken by Lee in at.% are (i) A1 is 75.38 Fe–14.9 Ni–9.72 Cr, (ii) A2 is 73.49 Fe–14.65 Ni–5.77 Cr–6.09 Al and (iii) A3 is 74.59 Fe–14.69 Ni–4.41 Cr–2.21 Al–4.09 Si.

SUS304 had comparatively less silicon as well as other impurities including Mo and Cu (refer Table 3). Azad et al. [39] had measured the activities of metals in SS304 using a novel technique developed by them [45]. The technique involved measurement of EMF of a galvanic cell with meta-stable coexistence of phases. The technique was referred to as a 'Meta-stable EMF method' (MEMF) by the authors. The calculated values of activities for Fe, Cr and Mn were compared with those obtained from experimental measurements reported by Azad et al. [39] and Hirai et al. [44] as shown in Fig. 2. The activity so computed for Fe is seen to be in excellent agreement with that from MEMF. The predicted a_{Mn} is seen to increase gradually with temperature while that reported by Hirai et al. remained constant over the temperature range employed in the KCMS and the numerical values are reasonably close to those predicted by the model. However, Azad et al. [39] observed sharp increase in a_{Mn} with increase in temperature. The values of a_{Cr} reported by Azad et al. are slightly more positive than the once predicted by the model. Nonetheless, the values reported by Hirai et al. are significantly more positive besides exhibiting steep variation with temperature. Hirai et al. have concluded that the high activity coefficients of Cr might be due to the formation of chromium carbide at the grain boundaries. Generally, atypical and abnormally high positive values of Cr activities reported in the literature were attributed to the formation of carbides of Cr. These values often reflected the realistic and non-equilibrium nature experienced by the multi component and multiphase materials. At very high temperatures viz., above 1350 K, carbides should redissolve into the alloy matrix and the multi component alloy should be tending close to equilibrium. However, at lower temperatures (viz., in the measurement range of MEMF) kinetic factors dominate over the conditions for equilibrium and thus resulting in non-equilibrium values. In this regard, the values of a_{Cr} reported by MEMF are not significantly different from the ones predicted by the model. However, values of a_{Ni} predicted by the model could be seen to be significantly different from those obtained by Azad et al. [39]. In general, it could be noticed from the Fig. 2, that computed activities of Fe varied marginally with minor compositional variations even in the different heats of otherwise same type of stainless steel namely SS304. This spread of values in the activities due to a corresponding spread in those of composition could contribute an error-band for any experimental measurement. In addition, there could be contributions arising from systematic experimental errors. One such systematic error could be due to the effect of oxygen present in trace levels in the KCMS system, which could cause different degrees of surface oxidation of the alloy samples as compared to the pure element used as the reference. The problems arising out of oxidation in the KCMS technique applied for the activity determinations were duly recognised by Hilpert [46]. It is well known that the pure metals such as Fe, Cr and Mn have a rather high propensity for surface-oxidation at higher temperatures. But the same elements exhibit considerably diminished reactivity in the alloyed form. These differential surface-oxidation characteristics

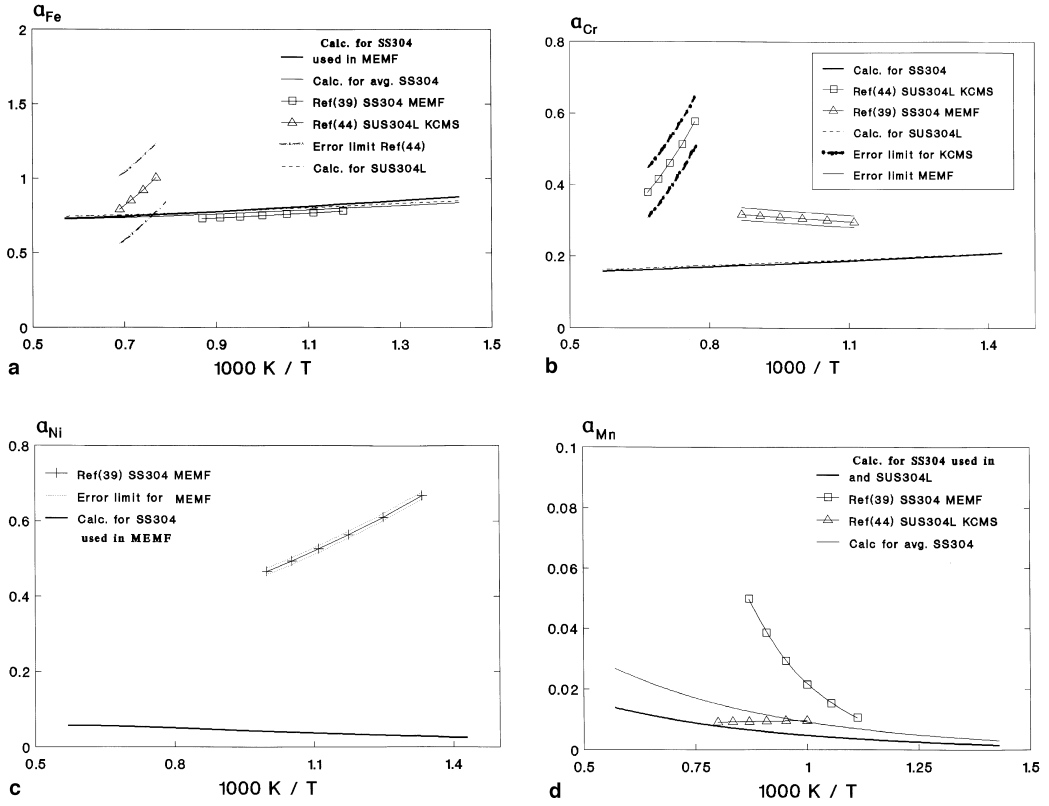

Fig. 2. Comparison of calculated activities in SS304 and SUS304L with corresponding experimental activity data from MEMF by Azad et al. [39] and KCMS by Hirai et al. [44]: (a) for Fe, (b) for Cr, (c) for Ni and (d) for Mn.

could explain anomalously high values of activity of some of these elements as reported by the KCMS technique. In general, activities obtained from KCMS are found to vary rapidly with in a small temperature range of measurements. Perhaps, this could be due to the surface depletion occurring at the time of measurements. In addition, there could be reaction between the container material of K-cell and the vapour phase thereby altering the activities of certain constituent elements. The MEMF technique is also observed to be limited with respect to applications to a number of elements and by a narrow temperature range of measurements. It is also possible that it may give the best results for some elements, while for a few others the results could be quite erroneous. Except for a_{Ni} and a_{Mn} in MEMF and a_{Cr} in KCMS, most of the other results from these techniques are in reasonably good agreement with the computed activities.

3.3. Comparison of SS316 and related materials

Koyama et al. [47] determined activities of metals in SS316 using KCMS technique over the range 1062–1380 K with LiCl as an internal standard in an alumina-lined molybdenum K-cell. They also determined surface concentration of constituent elements of SS316 by using auger electron spectroscopy (AES). Azad et al. [39] extended their technique to the measurements of activities of Fe, Cr, Ni, Mn and Mo in SS316 and 316LN and those of Fe and Cr in D9. Venugopal et al. [48] determined the activities of Fe, Cr, Ni and Mn in SS316 over the range 1293–2128 K with Ag as the internal standard over the same temperature range by using a K-cell made of Ta. However, Venugopal et al. and Koyama et al. [47] had made use of small pieces of stainless steel instead of fine powder samples which might restrict the attainment of equilibrium in the solid phase. The values of activities of Fe and Mn a_{Fe} and a_{Mn} reported by Koyama et al. are in agreement with the computed values presented in Fig. 3 within the limits of error-band attributed by them to the KCMS technique. For the surface composition of SS316 reported by Koyama et al., the present authors calculated the a_{Fe} and a_{Cr} making use of the newly developed model for the ferritic steels [49] and found the values to be in excellent agreement with those recomputed by Koyama et al. (after recognition of change in

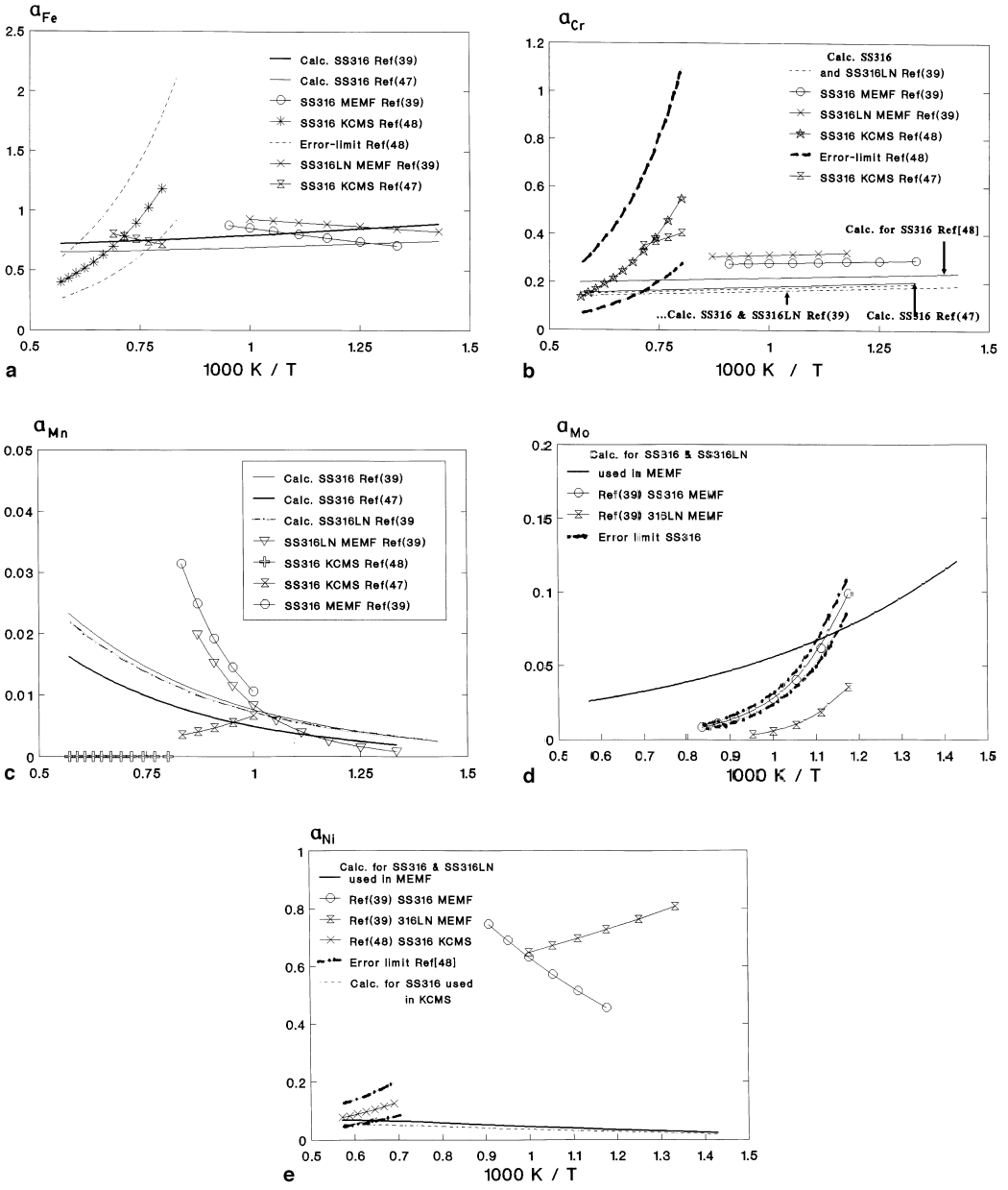

Fig. 3. Comparison of predicted activities with corresponding experimental data from MEMF by Azad et al. [39] and KCMS by Koyama et al. [47], Venugopal et al. [48]: (a) for Fe, (b) for Cr, (c) for Mn, (d) for Mo and (e) for Ni in SS316. (Please note from Table 4 that there is a small difference in the alloy composition, even though both groups have studied SS316.)

surface composition) as shown in Fig. 4. The values a_{Fe}, a_{Mo} and a_{Mn} are relatively close to the ones obtained from the MEMF technique by Azad et al. for SS316 (cf. Fig. 3). However, the values of a_{Fe} and a_{Cr} from Venugopal et al. [48] showed comparatively very sharp increase even within a narrow range of temperature. However, the values of a_{Mn} reported by them are in complete disagreement with those reported have for the same reasons as given above. In fact Koyama et al. [47] observed surface depletion of Mn which made them to restrict the maximum temperature for activity measurement to 1143 K.

Furthermore, the calculated a_{Mo} is in reasonably close agreement with that reported for SS316 by Azad et al. (Fig. 3(d)). However, the predicted activities for SS316LN are comparatively more positive than the ones

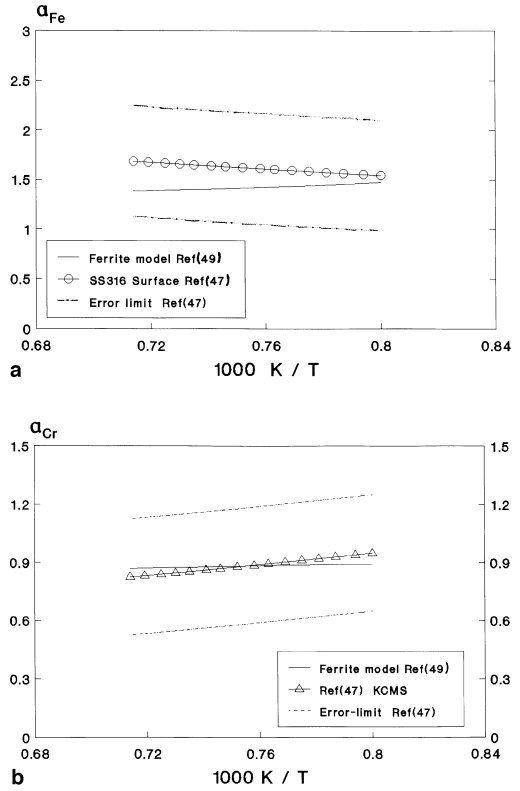

Fig. 4. Comparison of predicted activity coefficients for Fe and Cr using the model under development [49] with corresponding experimental data at the surface for SS316 samples observed by by Koyama et al. [47] using Auger electron spectroscopy (a) for Fe and (b) for Cr.

given by Azad et al. (cf. Fig. 3(d)). Nonetheless, the computation reveals a clear trend of rapid raise of a_{Mo} with decreasing temperature and similar trend was observed by Azad et al. for SS316. However, the disagreement is rather large between the computed values of a_{Mo} with the corresponding ones from MEMF in the case of SS316LN. The cause for the disagreement could be ascribed to the role played by nitrogen enriched surface layers. Even though the computed a $_{Ni}$ is completely in disagreement with that by the MEMF method, it is in close agreement with experimental results by Venugopal et al. (cf. Fig. 3(e)). This very large difference could be attributed to the possible direct displacement reaction between Fe in the stainless steel grains and NiF_2 instead of the electrochemical equilibrium between $[Ni]_{SS}$ and NiF_2.

3.4. Comparison of Ni-rich alloys

Hilpert [50] measured the activities of Fe, Cr, Ni and Co in heat exchanger materials viz., Nimonic alloy, Inconel and IN-643 by using KCMS over the temperature range 1350–1530 K with a K-cell made of W. The computed values of activities of Ni and Fe are in close agreement (within the experimental errors) with those from KCMS (cf. Fig. 5), whereas values of predicted activities for Cr and Co could be seen to be notably different from those obtained by Hilpert (cf. Fig. 6). The deviation from the ideal solution behaviour in the case of Cr was attributed by the investigator to the chromium carbide formation. The disagreement between the predicted and measured values in the case of Co could be attributed to the probable role of differential surface oxidation as cited by Hilpert [46].

4. Limitations of the model

The model assumed the composition of the alloy to be uniform and it would be the same as that of the bulk. As observed by Koyama et al. [47] the surface composition could be completely different from that of the bulk owing to the segregation of some elements at the surface. Hence, a knowledge of surface composition of these alloys would be indispensable. As mentioned earlier, the model assumed substitutional solution, the elements that occupied the interstitial position should be very low in concentration. Generally, many minor elements such as N, C, B and P were found to segregate at the grain boundaries under the thermal ageing process of the stainless steels resulting in the formation of different phases such as carbides, phospides and carbo-nitrides. Such non-uniform and multi-phase material should not be treated as a single fcc solid solution phase of homogeneous composition. This could be one of the serious limitations in the present approach. Binary interaction parameters which were optimised in the form of sub-regular solution selected for calculations. There could be some error in the optimisation of values in each binary system. Likewise, there could also be some errors arising from the choice of Kohler method instead of resorting to the ones such as Bonnier and Toop and Colinet methods [4]. In addition, each binary system could be best represented by one such method but not necessarily by the sub-regular solution model. However, choice of a single optimisation method for binary interaction parameters for all the binary systems under consideration could result in an unavoidable error component. Further, the method chosen had made use of only binary interaction energy terms without taking into account other higher order interaction parameters, besides facilitating computations for a large number of solute elements presently numbering up to 15. Therefore, whenever the higher order interaction parameters played a significant role, the prediction could be misleading. It should be stated that some of the investigators who optimised the binary systems had equated the interaction parameters for the bcc structure with those for the fcc structure.

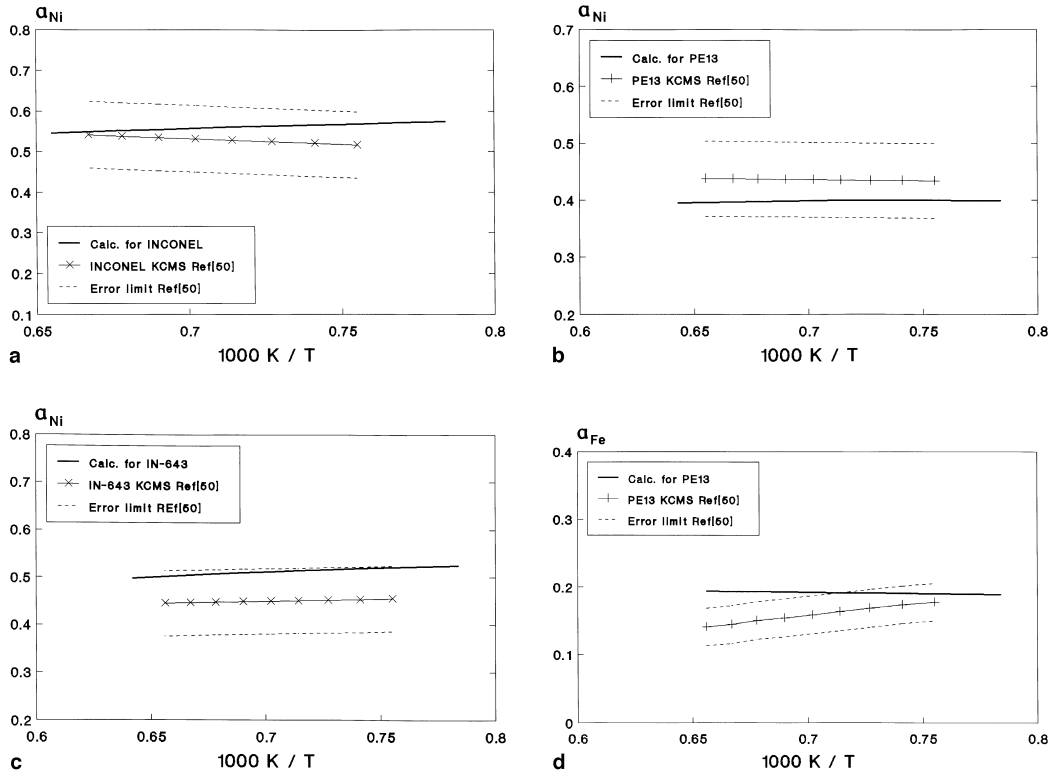

Fig. 5. Comparison of predicted activities with corresponding experimental data from KCMS by Hilpert [50]: (a) for Ni in Inconel, (b) for Ni in PE13, (c) for Ni in IN-643 and (d) for Fe in PE13.

This route was adopted in our present computations whenever the fcc interaction parameters were not available. Perhaps, the better approach could have been the one where in the fcc interaction parameters could be estimated using the fundamental physical principles as in pair-potential model or in the 'ab initio' calculations considering fcc structure for each congruous binary. However, such involved calculations should be again validated with proper experimental data.

5. Applications

Austenitic stainless steels are vital structural materials in Fast Reactors. Many properties of these structural materials could undergo significant modifications under conditions of irradiation in the nuclear reactors. In this context, a detailed knowledge of activities of metals in the zones influenced by the radiation-induced segregation (RIS) and radiation-induced precipitation (RIP) would be helpful in understanding the possible high temperature corrosion pathways that could occur in FBRs as by way of fuel-clad or clad-coolant chemical interactions. With the above mentioned goal, the present thermodynamic model is under development in order to predict the activities of each constituent element for any given composition of the austenitic alloy and possible applications of the model to RIS/RIP-influenced zones [51].

Despite, the inherent limitations of the present method, its genesis is from binary excess Gibbs energies. Hence, the predictions from the present model emanates from a more fundamental basis and as such even an order of magnitude agreement with experimental data should be considered as acceptable. In other words, the model may be used to examine the experimental results on the activities of metals in the stainless steel-related materials and pave a way for a deeper understanding of interaction energies in such multi-component systems. Further, the physical processes associated with grain boundary or surface modification due to secondary phase formation caused by precipitation/segregation could also be understood with the help of the data so generated. In addition, the model could also be used to predict the activities of minor elements such as Ta, Nb, Al, Cu, Co and V and their role in modifying those of major elements namely Fe, Cr or Ni. It is clearly evident from most of the figures referred earlier, the same material viz., SS316 or SS304 with very small changes in the concentrations of constituent elements could change the activities of all the elements to a certain extent. The

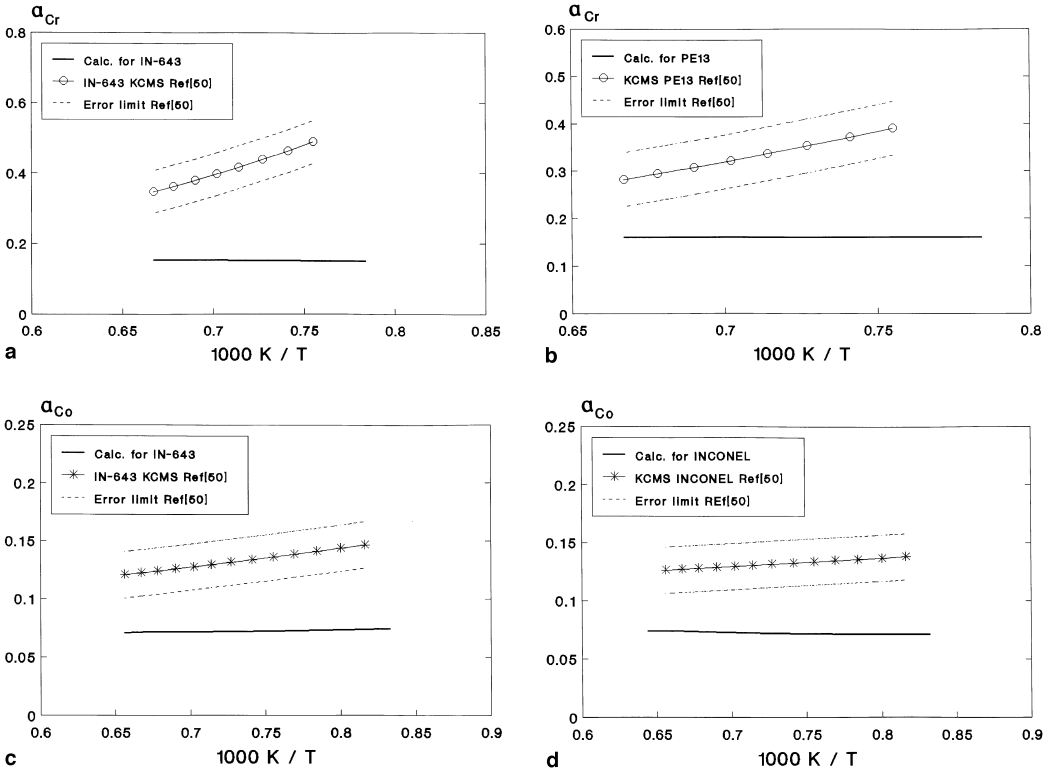

Fig. 6. Comparison of computed activities with corresponding experimental data from KCMS technique by Hilpert [50]: (a) for Cr in IN-643, (b) for Cr in PE13, (c) for Co in IN-643 and (d) for Co in Inconel.

model also could be utilised in numerical simulation of the effect of variation in each solute concentration in the stainless steel related materials. Fig. 7(a) illustrates the effect of the variation in nickel concentration on the activities of Fe, Cr, Mo and Ni at 1000 K for the initial composition corresponding to SS316. However, one should be guided by the existing high temperature phase diagram of Fe–Cr–Ni ternary [33,52] with information on the Cr and Ni equivalents [53] in order to ascertain whether the composition selected for the computation lies in the austenitic regime. The model shows that the values of γ_{Fe}, γ_{Ni} and γ_{Cr} vary marginally with the increase in Ni content up to 30 at.%. However, the value of γ_{Mo} and γ_{Mn} diminish asymptotically with the increasing Ni concentration. It is interesting to note that the effect of Ni on the activity-coefficients of minor elements could be analysed meaningfully by using the present model. For instance, the relatively high values of the activity coefficient of a given element suggests that the element is in the most reactive form whereas the much lower ones suggest that the said element is stabilised in the matrix.

In an attempt on numerical simulation the role of Si concentration could be examined for a SS316 alloy with [Si] varying between 0.2 and 6 at.% on the γ of Fe, Cr, Ni, Mo and Mn was examined and the typical results are presented in Fig. 7(b). The numerical simulation was restricted to 6 at.% Si in anticipation of the appearance of a second phase. The actual limiting concentration of Si should be obtained with the knowledge of Cr and Ni equivalents. These results depict a significant increase in the values of γ of Fe, Ni and Mo with increase in Si content. Curiously, the increase in γ_{Mo} is relatively much higher for a small change in the concentration of Si. For example, the value of γ_{Mo} increased from ~4 to 6 corresponding to an increment of Si from 0.2 to 6.2 at.%.

The line of approach adopted in this paper is somewhat similar to the one by Sigworth and Elliott [54] (of course whose work was related to dilute liquid iron alloys). Nevertheless, this paper provides the algebraic expressions for the interaction parameters, in order to facilitate modifications for incorporation of new interaction parameters updated from time-to-time.

6. Conclusions

1. A thermodynamic model based on sub-regular solution is presented to assist in the prediction of high temperature activities of major constituent elements

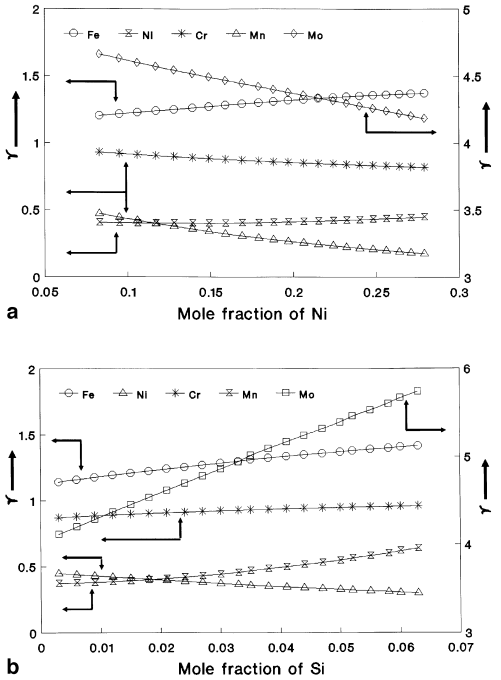

Fig. 7. Numerical simulation of the effect of variation in the concentration of an alloying element content on the activity-coefficients of other constituents elements for the initial composition corresponding to SS316: (a) for Ni and (b) for Si.

in austenitic stainless steels and other iso-structural alloys.

2. A comparison between the activity coefficients predicted by the model and those reported from the available literature which were based on Knudsen cell mass spectrometric and meta stable EMF methods has shown a fair agreement between them.
3. The possible reasons for the mismatch in the values of activity coefficients are discussed in terms of limitations of our thermodynamic modelling (such as choice of the model or non-availability of higher order interaction energies) and the likely errors in experimental measurements.
4. The application of the model for simulation studies involving variation of composition with respect to one solute element is also presented.

Acknowledgements

The authors are grateful to Dr V.S. Raghunathan Associate Director, Material Characterisation Group, Dr Baldev Raj, Director, Metallurgy and Materials Group and Dr Placid Rodriguez, Director, IGCAR for their keen interest and constant encouragement throughout the course of this work. The work reported here would form a part of the PhD thesis to be submitted by H.P. Nawada to the University of Madras.

References

[1] L. Kaufman, H. Nesor, Metall. Trans. 5A (1974) 1623.
[2] M. Hasebe, T. Nishizawa, Application of phase diagrams in metallurgy and ceramics, Proc. NSB workshop, Gaitherburg, USA, vol. 2, 1977, p. 911.
[3] L. Kaufman, H. Bernstein, Computer Calculation of Phase Diagram, Academic Press, NY, 1970.
[4] I. Ansara, Int. Metal Rev., The Metall. Soc. London 1 (1979) 20.
[5] M. Hillert, L.I. Staffanssson, Acta Chem. Scand. 24 (1970) 3618.
[6] L. Kaufman, H. Nesor, Z. Metallkd. 64 (1973) 249.
[7] J.O. Anderson, B. Sundamen, Calphad 11 (1987) 83.
[8] L. Kaufman, H. Nesor, Calphad 2 (1978) 55.
[9] D.D. Hughes, L. Kaufman, Calphad 3 (1979) 175.
[10] L. Kaufman, Calphad 3 (1979) 45.
[11] L. Kaufman, H. Nesor, Calphad 2 (1978) 295.
[12] L. Kaufman, Calphad 2 (1978) 117.
[13] L. Kaufman, Calphad 15 (1991) 243.
[14] M. Hasebe, T. Nishizawa, Calphad 5 (1981) 105.
[15] J.O. Anderson, Calphad 7 (1983) 305.
[16] D. Perrot, J.Y. Dauphin, Calphad 12 (1988) 33.
[17] M. Grujicic, I. Wang, W.S. Oven, Calphad 10 (1986) 37.
[18] L. Kaufman, Calphad 2 (1978) 81.
[19] L. Kaufman, H. Nesor, Calphad 2 (1979) 325.
[20] L. Kaufman, K. Taylor, Calphad 8 (1984) 25.
[21] K. Frisk, Calphad 15 (1991) 79.
[22] L. Kaufman, H. Nesor, in: N.B. Hanny (Ed.), Treatise on Solid State Chem., vol. 5, Plenum, New York, 1975, p. 179.
[23] W. Huang, Calphad 15 (1991) 195.
[24] M. Grujicic, I. Wang, W.S. Oven, Calphad 10 (1986) 117.
[25] M. Jarl, Scand. J. Metall. 7 (1978) 93.
[26] L. Kaufman, Calphad 15 (1991) 261.
[27] J.C. Lee, Y.Y. Chaung, K.C. Hsiels, Y.A. Chang, Calphad 11 (1987) 73.
[28] M. Hämäiäinen, K. Jääskeläinen, R. Luoma, M. Nuotio, P. Taskinen, O. Teppo, Calphad 14 (1990) 125.
[29] B. Uhrenius, L. Kaufman, Calphad 3 (1979) 223.
[30] M.H. Ohtani, M. Hillert, Calphad 15 (1991) 73.
[31] K.C. Harikumar, P. Wollants, L. Delaey, Calphad 8 (1994) 71.
[32] L. Kaufman, H. Nesor, in: R. Huggins (Ed.), Annual Review of Material Science, vol. 3, Annual Rev. Inc., Palo Alto, California, 1973, p. 1.
[33] T. Chart, F. Putland, A. Dinsdale, Calphad 4 (1980) 27.
[34] J.O. Anderson, N. Large, TRITA-MAC-0322, Royal Inst. of Tech., Stockholm, Sweden, 1986.
[35] B.J. Lee, S.K. Lee, D.N. Lee, Calphad 11 (1987) 253.
[36] J.L. Murry, Bull. Alloy Phase Diag. 2 (1981) 320.
[37] A.T. Dinsdale, Calphad 15 (1991) 317.
[38] Metals Handbook, 8th ed., vol. 7, American Society for Metals, Metals Park, OH, 1972, p. 132.
[39] A.M. Azad, O.M. Sreedharan, C. Narayanan, J.B. Gnanamoorthy, Scand. J. Metall. 21 (1992) 223.

[40] S.W. Gibby, G.R. St. Pierre, Trans. Metall. Soc. AIME 245 (1970) 1749.
[41] G.R. Belton, R.J. Fruehan, Metall. Trans. 1 (1970) 781.
[42] H. Probst, KH. Geiger, E. Münstermann, Z. Metallkd. 70 (1979) 798.
[43] M.C. Y Lee, J. Nucl. Mater. 167 (1989) 175.
[44] M. Hirai, A. Akito, M. Yamawaki, M. Kanno, J. Nucl. Sci. Technol. 20 (1983) 333.
[45] A.M. Azad, O.M. Sreedharan, J.B. Gnanamoorthy, J. Nucl. Mater. 144 (1987) 94.
[46] K. Hilpert, J. Nucl. Mater. 80 (1980) 126.
[47] T. Koyama, M. Kanno, M. Yamawaki, Mass Spectros. (Shitsurobunseki) 35 (1987) 56.
[48] V. Venugopal, S.G. Kulkarni, C.S. Subbanna, D.D. Sood, J. Alloys Compounds 218 (1995) 95.
[49] H.P. Nawada, O.M. Sreedharan, to be published.
[50] K. Hilpert, Thermodynamics Nuclear Materials, 1979, IAEA, Vienna, 1980, IAEA-SM-236/27, p. 61.
[51] H.P. Nawada, O.M. Sreedharan, J.B. Gnanamoorthy, Proceedings of the Symposium on Localised Corrosion and Environmental Cracking (SOLCEC), by Indian Institute of Metals, Kalpakkam Chapter, India, January 1997, p. C56.
[52] P. Marshall, Austenitic Stainless Steels, Microstructure and Mechanical Properties, Elsevier, London, 1984.
[53] D.R. Harries, Physical metallurgy of Fe–Cr–Ni austenitic steels, Mechanical behaviour and nuclear applications of stainless steels at elevated temperatures, Int. Conf. Mech. Behaviour and Nucl. Applications of Stainless Steel at Elevated Temperatures, Varese, London Metal Society, May 1981.
[54] G.K. Sigworth, J.F. Elliott, Met. Sci. 8 (1974) 298.